بسم الله الرحمن الرحيم

Sudan Academy of Sciences (SAS)
Atomic Energy Council

Quality control for some digital fluoroscopy equipment used in Sudan

By

Abdalrhman Ibrahim Nayl Edam

A thesis submitted in partial fulfillment of the requirements for the degree of Master of Medical Physics

Supervisor: Dr. Ibrahim Idris Suliman

July 2009

Sudan Academy of Sciences

Atomic Energy Council

Examination committee

Title	Name	Signature
External Examiner	Dr. Farouk Idris Habbani	
Supervisor	Dr. Ibrahim Idris Suliman	
Academic Affairs Representative	Mr. Ammar Mohammed Elamin	

Dedication

To my mother, my father, brothers and to all my friends

Acknowledgments

I would like to express my sincere thanks and appreciation to my supervisor Dr. Ibrahim Idris Suliman for his guidance, encouragement and advice throughout the course of this project. Without that this work would be extremely difficult.

I am also extremely grateful to Nada Abbas for her valuable assistance, suggestion and cooperative work during the whole period of the project.

Abstract

The aim of this work was to perform quality control (QC) for six digital fluoroscopy units used for cardiovascular and interventional radiology procedures. Measurements were based on the QC protocol developed in the framework of European Commission (EU) DIMOND III project.

Measurements made included: beam quality (half-value layer, HVL), peak tube voltage (kVp) accuracy, automatic exposure control(AEC) and patient dose in terms of entrance surface air kerma rate plus image intensifier input air kerma rate. Dose measurements were made using Calibrated dose rate meter. Field limitation and source to skin distant measurements in addition to evaluation radiation protection tools for occupation exposure were performed. Image quality was evaluated in terms of spatial resolution and Contrast detail detectability. Patient dose measurements was performed using polymethylmethacrylate (PMMA) patient equivalent phantom whereas image quality was assessed using Huettner Type 53 spatial frequency grating and TO10 contrast detail phantom.

The results show that the measured HVL and peak tube voltage were within the recommended limits of 10 % in four fluoroscopy units. Entrance surface air kerma rate measured ranged from 6.1 to 250 mGy/min for fluoroscopy units operated in pulsed, continuous and cine mode of operation. These results were obtained using varying thicknesses of PMMA phantom. Most values are in reasonable agreement with internationally established reference levels with exception to one fluoroscopy unit where doses were remarkably high. Field limitation and minimum source to skin distance were well within the recommended limits of 30 cm for all fluoroscopy units. The limiting resolution was ranged from1.0 to 2.2 LP /mm for image intensifier field diameters between 7 and 23 cm. The results of present study can be used as baseline for future quality assurance measurements.

الخلاصه

كان الهدف من هذا البحث تقييم بعض اجهزه الاشعه المتفلوره المستخدمه فى السودان بولايه الخرطوم بأجراء قياسات ضبط الجوده عليها، وقد تضمن هذا العمل ست وحدات اشعه متفلوره فى خمس مستشفيات مختلفه بولايه الخرطوم ،وقد كانت هذه الوحدات تسخدم فى عمليات جراحه القلب والقسطره وبعض العمليات الاخرى التى تتطلب المراقبه بواسطه الاشعه السينيه .

كانت خطه العمل فى قياسات ضبط الجوده على هذه الست الوحدات مستنده على برتكول طور بواسطه الهيئه الاوربيه(EU) فى مشروع سمى بمشروع دايموند ثلاثه (DIMOND III) وقد تضمنت القياسات كل من: فرق الجهد المطبق على الانبوب المولد للاشعه السينيه(kVp) ، جوده الحزمه الاشعاعيه بواسطه قياس السمك المنصف للقيمه(HVL)، التحكم الالى لانتاج الاشعه السينيه(Auto Exposure Control)، معدل الجرعه الاشعاعيه السطحيه للمرضى الناتجه عن استخدام الاشعه السينيه فى العمليات (Entrance Surface Air Kerma rate) حدوديه الحقل الاشعاعى على مستقبل الاشعه(Field Limitation) ، معدل كميه الاشعه الساقطه على مستقبل الاشعه(Image Intensifier Air Kerma Rate)، جوده الصوره (Image Quality) ، اقل مسافه من بؤره الاشعه حتى الجلد (Source to skin Distance) ووسائل الوقايه من الاشعاع(Radiation Protection) .

القياسات تمت باستخدام غرفه اشعه معايره(Calibration Ionization Chamber) لقياس معدل الجرعه وشرائح من ماده(PMMA) كثافتها مكافئه لكثافه الانسجه البشريه لمحاكات شكل المريض، بعض الادوات لقياس جوده الصوره مثل(Huttner type 53 and TO10) .

النتائج اظهرهت ان وحدات الاشعه تعمل بصوره جيده. وقد كانت الاخطاء فى القياسات داخل حدود الاخطاء المسموح بها عالميا مع الاثتثناء لبعض الوحدات فى الاختبارات المتعلقه ب: فرق الجهد المطبق على الانبوب و معدل الجرعه السطحيه.

تبين من خلال العمل ان كل هذه الوحدات لم يقام بأجراء قياسات ضبط الجوده لها من قبل وان القياست التى اجريت يمكن ان تكون كمرجع لقياسات ضبط جوده مستقبليه لهذه الوحدات.

Table of Contents

List of Figures

List of Tables

Abbreviation

QA	Quality Assurance
QC	Quality Control
IR	Interventional Radiology
Irish	Ireland
DSA	Digital Subtraction Angiography
DSI	Digital Spot Image
EU	European
HVL	Half -Value Layer
kVp	kilo volt peak
mAs	milli ampere second
Gy	Gray
ABC	Automatic Brightness Control
ESD	Entrance Surface Dose
PMMA	Polymethylmethacrylate
Lp	Line Pair
IQF	Image Quality Figure
FPD	Flat Panel Detector
II	Image Intensifier
MED	Medical Exposures Directive
AEC	Automatic Exposure Control
RP	Radiation Protection
EDR	Entrance Dose Rate
XRII	X-Ray Image Intensifier
FOV	Field Of View
KAP	Kerma Area Product
DAP	Dose Area Product
ESAK	Entrance Surface Air Kerma
TCDD	Threshold Contrast Detail Detectability
IPEM	Institute of Physics and Engineering in Medicine
UV	Ultra Violet
SI	Standard International
MESD	Maximum Entrance Surface Dose

TLD	Thermo luminescence dosimeter
NRPB	National Radiation Protection Board
FID	Focal to Image Distance
FSD	Focal to Skin Distance
ROC	Receiver Operating Characteristic
MTF	Modulation Transfer Function
K	Large-area signal transfer
NPS	Noise Power Spectrum
NEQ	Noise Equivalent Quanta
DQE	Detective Quantum Efficiency
ROC	Receiver Operating Characteristic
SNR	Signal to Noise Ratio
MAFC	Multiple Alternative Forced Choice
CT	Computed Tomography
PPS	Pulse Per Second

Chapter One

Introduction

Diagnostic and interventional radiology encompass indispensable tools in the modern health care. Substantial dose and skin injuries were reported in the literature from digital and interventional radiology procedures [1].

Quality control (QC) has been acknowledged as a powerful and effective tool in optimizing radiation protection of the patients in diagnostic and interventional radiology (IR). Equipment performance testing is necessary to meet the aims of diagnostic radiology, i.e. to obtain images adequate for the clinical purpose with minimum radiation dose to patient. QC in conventional diagnostic radiology has been well established. However, QC of modern digital radiology systems requires different approaches owing to differences in image receptor, image display devices, image format and equipment configuration. Available QC testing methods should be updated to encompass the developments in the field and to include digital imaging systems. Recently, and as of the European Commission research project DIMOND III, a protocol has been developed for quality control of equipment used in digital and interventional radiology [2] .The validity of the DIMONDIII protocol has been tested and acceptable results were demonstrated [3].

QC measurements in the present study were performed based on DIMOND III protocol.

1-1-Objectives:

To perform QC measurements on fluoroscopy units used for cardiovascular and other interventional radiology procedures.

To use QC measurements results for optimizing fluoroscopically guided procedures.

To measure patient dose and image quality using DIMOND III quality control protocol.

1-2-Literature review:

Digital fluoroscopy quality control measurements [4]:

In this work quality control (QC) was performed on three digital fluoroscopy systems used for cardiovascular, digital subtraction angiography (DSA) and digital spot imaging (DSI). Measurements were based on the QC protocol developed in the framework of European Commission (EU) DIMONDIII project. For digital fluorography system used for DSI, measurements included were beam quality (half-value layer, HVL), peak tube voltage (kVp) accuracy and reproducibility, tube-current exposure-time product (mAs) linearity and automatic brightness control (ABC). Patient dose and image quality were measured for the two digital fluoroscopy systems using a patient equivalent phantom. Spatial resolution was measured using the Huettner Type 53 spatial frequency grating. A contrast detail phantom CDRAD 2.0 was used to measure the threshold contrast detail performance.

The results obtained showed that the measured HVL and peak tube voltage were within the recommended limits of 10 %. Maximum patient entrance surface dose (ESD) rate of 27.8 mGy/min, 46.5 mGy/min and 84.1 mGy/min were measured using a 20 cm thick polymethylmethacrylate (PMMA) phantom at the cardiovascular unit operated in low, normal and high dose mode of operation, respectively. ESD rate of 28 mGy/min and 42.2 mGy/ min were measured using a 20 cm thick PMMA phantom at the DSA unit operated in pulsed and continuous mode of operation, respectively (lowest value should be for pulsed mode). The results of this study were in reasonable agreement with internationally established reference levels.

The median limiting resolution was 1.6 Lp/mm for image intensifier field diameters between 14 and 38 cm. Mean low contrast resolution expressed as image quality figure (IQF) was 107.

The results obtained by the authors for incident air kerma rate measured for digital fluoroscopy are consistent with the recommended values when fluoroscopy is operated in pulsed mode. These values were often exceeded with continuous and high dose rate mode.

Acceptance testing of fluoroscopy systems used for interventional purposes [5]:

In this work the authors performed acceptance testing on 18 fluoroscopy installations (interventional II/TV, interventional FPD, and mobile C-arm II/TV) in a number of Irish hospitals from 1999 to 2008.

Acceptance testing and routine quality assurance (QA) of X-ray systems are the requirements of the EU Medical Exposures Directive (MED) and these requirements were subsequently implemented into Irish legislation. The MED states that special consideration should be given to the QA and dose assessment of high dose procedures such as interventional fluoroscopy.

QC tests performed include: Tube and generator performance, automatic exposure control (AEC) entrance doses, image quality, electrical safety, mechanical safety, RP and equipment design.

The authors stated that, all systems were found to have failed one or more acceptance tests. Dose rate, image quality and RP issues were identified on the majority of systems tested. About 50% of systems tested were found to have significant issues requiring action by equipment suppliers prior to the system going into clinical use.

A comparison of entrance doses from a new vascular interventional FPD system Vs. two conventional vascular II/TV was done. All three systems were from the same manufacturer. Entrance dose measurements were performed in line with IPEM protocols. The results for doses in the fluoroscopy mode showed that patient EDRs made with a 20 cm water phantom were similar for all three systems (full field setting, normal flouro mode).

Detector EDR was highest on the FPD system. In the digital acquisition mode, the dose per frame at the FPD entrance was greater than that at the majority of interventional systems and greater than both conventional II/TV systems (on the same default clinical ‘dose’ setting).

Results from subjective image quality tests using standard Leeds test objects were comparable between the FPD and conventional II/TV fixed systems (noise, threshold contrast detail detectability and limiting spatial resolution). Spatial resolution was observed to be slightly greater on the FPD system (1.4 Lp/mm vs. 1.25 Lp/mm on both II/TVs). The FPD has a full field size diagonal of 48 cm and the II/TV systems have a field diameter of 40 cm.

The authors highlight the importance of comprehensive acceptance testing for complex modern fluoroscopy systems. The authors have found that it is beneficial to liaise with both the system applications' specialist and the clinical users prior to acceptance testing, to ascertain user's requirements and clinical settings. This will assist with the efficient testing of relevant modes of operation. The default clinical 'dose' setting should be optimized to ensure that it is as low as reasonably achievable. Comparative studies of new systems will assist the on-going development of testing guidelines and the criteria of acceptability for modern fluoroscopy equipment.

Soft-Copy Quality Control of Digital Spot Images Obtained by Using X-ray Image Intensifiers [6]:

In this work the authors have evaluated 12 X-ray image intensifier (XRII) digital spot systems.

There were four objective tests performed to assess (XRII) digital spots: entrance exposure, patient exposure, soft-copy gray scale, and pixel noise. Two additional tests were performed to assess high-contrast limiting resolution and threshold contrast detection.

The authors results showed that the Digital spot (XRII) entrance exposures averaged 1×10^{-7} C/kg (0.38 mR) for units with large fields of view (FOVs), mean entrance exposure in a medium-size patient was 1.25×10^{-5} C/kg (48 mR). Also luminance measurements of the table-side monitors provided a mean of 473 just-noticeable differences in gray scale with the room lights off. Mean resolution with a bar test pattern was measured as 1.5 line pairs per millimeter for systems with a 40-cm FOV. Measured pixel noise (in relative units) was 6–25. Mean threshold contrast with the lights off was 0.85%.

The authors study concluded that once input exposure was normalized for FOV and image matrix size, soft-copy assessment of limiting resolution with either low-contrast detection or, preferably, an off-line noise metric (pixel SD) provides objective measurements of digital spot image quality. With the lights on, 10 systems with room-light sensors had an 11% loss of gray scale. For systems without sensors, the loss was 33%.

Survey on performance assessment of cardiac angiography systems [7]:

The aim of the authors study was to assess the performances of different cardiac angiographic systems. A questionnaire was sent to centers participating in SENTINEL Project to collect dosimetry data (typical entrance dose rate in fluoroscopy and imaging mode), image quality evaluations (low and high contrast resolutions) and KAP (kerma area product) calibration factors. There results from that survey

could contribute to the explanation of patient dose variability in angiographic cardiac procedures and to derive reference levels for cardiac angiographic equipment performance parameters. Tests included measurement of air kerma dose rates in fluoroscopy and digital acquisition modes and a subjective assessment of image quality using the Leeds test object (TOR 18FG). Dose rates were measured under automatic exposure control in fluoroscopy and digital acquisition modes measured the entrance surface air kerma rate with a phantom of 20 cm PMMA thickness to simulate a patient attenuation, and the field of view (FOV) on the detector had been sited at 22 cm or nearest with a focus-entrance phantom distance of 65 cm and the image detector positioned at 5 cm from the exit phantom surface. With the purpose to use the KAP meter calibration factor to correct collected patient KAP values, the calibration procedure was performed taking into account the attenuation determined by the patient table and mattress. The calibration had been performed at 60–80–100 kV X-ray qualities with an ion chamber on the axis of the X-ray beam placed at minimum 10 cm away from the patient table and the image detector to avoid scatter. The different X-ray qualities were reached by inserting in the X-ray beam between the ion chamber and the image detector, attenuating material (copper and/or aluminum) simulating the patient attenuation with both kilo volt and added filtration use to typical clinical conditions. Surface area was calculated from field dimensions measured with a radio-opaque ruler or an equivalent method. KAP calibration factor was assumed as the mean value of the calibration factor measured for the three X-ray qualities.

The authors survey on the cardiac angiographic units in a sample of European centers demonstrates a large variability in entrance dose rates for fluoroscopy and image acquisition modes, image quality performance and KAP calibration. As an outcome of the study, a preliminary set of reference levels for the ESAK quantity was proposed, which can be adopted by centers and maintenance engineers to set up cardiac equipment at an acceptable dose performance level and by standardization bodies as an input to introduce proper standards. SENTINEL consortium is finally recommended as a European action directed to harmonize the level of performance of angiographic systems used in the daily cardiac practice.

Threshold contrast detail detectability curve for fluoroscopy and digital acquisition using modern image intensifier system [8]:

The authors study was to present updated TCDD curve for fluoroscopy and new curve for digital acquisition. The images of this test were acquired under standard reproducible exposure conditions,

which allow the contrast of the details to be known and which facilitate consistency by using TO10 to fluoroscopy and TO12 to acquisition contrast test object. The image reader scores the image by visually assessing the lower contrast detail visible for each group of the same diameter. The image intensifier input air kerma was measured using calibrated MDH 2025 electrometer with 60 cm^3 circular ionization chamber and copper filtration.

The authors results showed that the generation of TCDD curves from images of standard test object is simple procedure that allow analysis of image quality for a range of imaging modalities, including image intensifier systems and comparing between the fluoroscopic systems in acceptance test or in rotation quality control of image quality.

Subjective and objective measurements of image quality in digital fluoroscopy [9]:

The authors study was to compare between the physics and clinical assessment of image quality. Physics assessments were based on IPEM protocols using Leeds test objects. Clinical assessment was based on a questionnaire. A total of 15 systems in three European locations were assessed, covering a range of image intensifier-TV digital fluoroscopy units. Analysis of 274 clinical questionnaires showed that clinical and physics assessments did not place systems in the same order, based on a given image quality parameter. In almost all the comparisons, low level correlation was measured for statistical comparison of rank order ($rs<0.3$). However, broad agreement was observed between physics and clinical assessments for image quality associated with contrast and noise. The authors emphasized the importance of maintaining links with clinical assessment, when developing quality assurance metrics, and measuring the mutual performance of clinical and physical assessments of image quality.

Clinical and physics assessments based on questionnaire and test object measurements, do not place systems in the same order of merit based on a given image quality parameter. There was, however, evidence for broad agreement between physics and clinical assessments for image quality associated with contrast and noise. The results suggest that both groups judged the systems as operating well (‘average to good’), but disagreed on the ordering within this category. The study reflects the difficulties of image quality assessment and quality control in the field. It emphasizes the importance of maintaining links with clinical assessment when developing quality assurance metrics and of measuring the mutual performance of clinical and physical assessments of image quality.

Assessment of performance of new digital image intensifier fluoroscopy system[10]:

The authors work was to assess the physical parameters including image quality and patient dose rates on a recently installed digital fluoroscopy unit. The Digital Fluoroscopy was new for Bulgaria and there was a gap in the experience within the radiologists in exploring the advantages of this modality for imaging. At the same time in Bulgaria, Quality Assurance protocols in Digital Fluoroscopy does not exist and based on the findings obtained some initial recommendations are prepared. The purpose of these efforts was to propose optimization strategies for digital fluoroscopy of maintaining good diagnostic image quality at minimal patient doses. The modern fluoroscopy units are often automated and software controlled. In the work various users defined and automated modes were examined on an Axiom Icons R200 unit (Siemens, Germany) as respected image quality parameters and patient doses were measured, low and high contrast resolution were assessed for different field sizes and fluoro modes using Leeds type test objects. The Incident Dose rates were measured using standard 30x30 cm^2 PMMA phantom with thickness varying between 16 and 30 cm at different available filtrations, automatic brightness control curves, and pulsed fluoroscopy modes. The Incident Dose Rate (without backscatter) measured on 20 cm PMAA and largest field of view were from 2.9 to 4.0 mGy/min for the different dose modes available. The low contrast sensitivity varied from 1.3 to 1.8 %, as the limiting spatial resolution was changing from 1.6 to 2.8 Lp/mm for the available magnification and dose modes. The authors performance on systems showed a big potential for performance optimization in terms of image quality and dose. It completely satisfies Quality Control requirements applicable for conventional Image Intensifier systems. The results obtained can be used in two main directions - development of better optimized local practice standards and development of a quality control programmer relevant to digital fluoroscopy systems.

Quality control measurements for fluoroscopy systems in eight countries participating in the SENTINEL EU coordinator action [11]:

In SENTINEL work package 1 on functional performance and standards it was decided to organize and perform a trial on image quality and physical measurements. A survey on inventory of equipment and equipment standards was organized to collect information on equipment available for measurements in the trial, equipment available for toolkit to be used during the trial and protocols available for the measurements. Eight participants responded to the questionnaire. Equipment for the toolkit could be

made available by three participants. Among the protocols available for quality control of (digital) fluoroscopy systems the protocol developed by the Department of Medical Physics & Bioengineering, Dublin, Ireland appeared to be the most suitable. In addition, monitors could be checked using a software tool made available by the University of Leuven.
The SENTINEL toolkit containing equipment and instructions circulated among seven participants in the period August 2006 to October 2006. Due to problems related to customs (Bulgaria is not yet a full EU member state) the measurements in Bulgaria were made with local equipment.

1-3-Ionizing radiation:

Ionizing radiation consists of subatomic particles or electromagnetic waves that are energetic enough to detach electrons from atoms or molecules and thus ionizing them. The occurrence of ionization depends on the energy of the impinging individual particles or waves, and not on their number. An intense flood of particles or waves will not cause ionization if these particles or waves do not carry enough energy to be ionizing. Roughly speaking, particles or photons with energies above a few electron volts (eV) are ionizing. Examples of ionizing particles are energetic alpha particles, beta particles, and neutrons. The ability of electromagnetic waves (photons) to ionize an atom or molecule depends on their wavelength. Radiation on the short wavelength end of the electromagnetic spectrum of x-rays and gamma rays are ionizing. Ionizing radiation comes from radioactive materials, x-ray tubes, particle accelerators, and is present in the environment. It has many practical uses in medicine, research, construction, and other areas, but presents a health hazard if used improperly. Exposure to radiation causes microscopic damage to living tissue, resulting in skin burns and radiation sickness at high doses. However cancer tumors and genetic damage are also observed at low doses [12].

X-rays are a form of electromagnetic radiation. X-rays commonly used in medical application have a wavelength in the range of 10 to 0.01 nanometers, corresponding to energies of 40kV to 150kV in diagnostics procedures. They are shorter in wavelength than UV rays. In many languages, X-radiation is called Röntgen radiation after its first investigator, Wilhelm Conrad Röntgen, who had originally called them X-rays meaning an unknown type of radiation.

X-rays are primarily used for diagnostic radiography. As a result, the term X-ray is metonymically used to refer to a radiographic image produced using this method, in addition to the method itself. X-rays are a form of ionizing radiation and as such can be dangerous [12].

1-4-Dosimetric quantities and units:

Spatial dosimetric quantities and units are used to specify the amount of dose received by patient during diagnostic and interventional procedures, these units are:

1-4-1-kerma (K): is the quotient of dEtr by dm, where dEtr is the sum of the initial kinetic energies of all the charged particles liberated by uncharged particles in a mass dm of material, thus:

$$K = dEtr/dm \ldots\ldots\ldots\ldots\ldots\ldots\ldots\ldots (1\text{-}1)$$

The SI Unit is: J/kg, special name gray (Gy) [13].

1-4-2-kerma rate (ќ): is the quotient of dK by dt, where dK is the increment of kerma in the time interval dt, thus:

$$ќ = \frac{\mathrm{dK}}{\mathrm{dt}} \ldots\ldots\ldots\ldots\ldots\ldots\ldots\ldots\ldots\ldots (1-2)$$

The SI Unit is: (J/kg)/s, or Gy/s.

1-4-3-absorbed dose (D): can be used to quantify the deposition of energy by ionizing radiation. It is defined as the quotient of dε by dm, where dε is the mean energy imparted to matter of mass dm, thus:

$$D = \frac{d \in}{dm} \ldots\ldots\ldots\ldots\ldots\ldots\ldots\ldots\ldots\ldots\ldots (1-3)$$

The SI Unit is: J/kg, special name gray (Gy).

1-4-4-absorbed dose rate (Ď): is defined as the quotient of dD by dt, where dD is the increment of absorbed dose in the time interval dt, thus:

$$\check{D} = \frac{dD}{dt} \ldots\ldots\ldots\ldots\ldots\ldots\ldots\ldots\ldots\ldots\ldots\ldots\ldots (1-4)$$

The SI Unit is: (J/kg)/s, or Gy/s [13].

1-4-5-exposure (X): is defined as the quotient of dQ by dm, where dQ is the absolute value of the total charge of the ions of one sign produced in air when all the electrons and positrons liberated or created by photons in air of mass dm are completely stopped in air, thus:

$$X = \frac{dQ}{dm} \ldots\ldots\ldots\ldots\ldots\ldots\ldots\ldots\ldots\ldots\ldots\ldots\ldots (1-5)$$

The SI Unit is: C/kg [13].

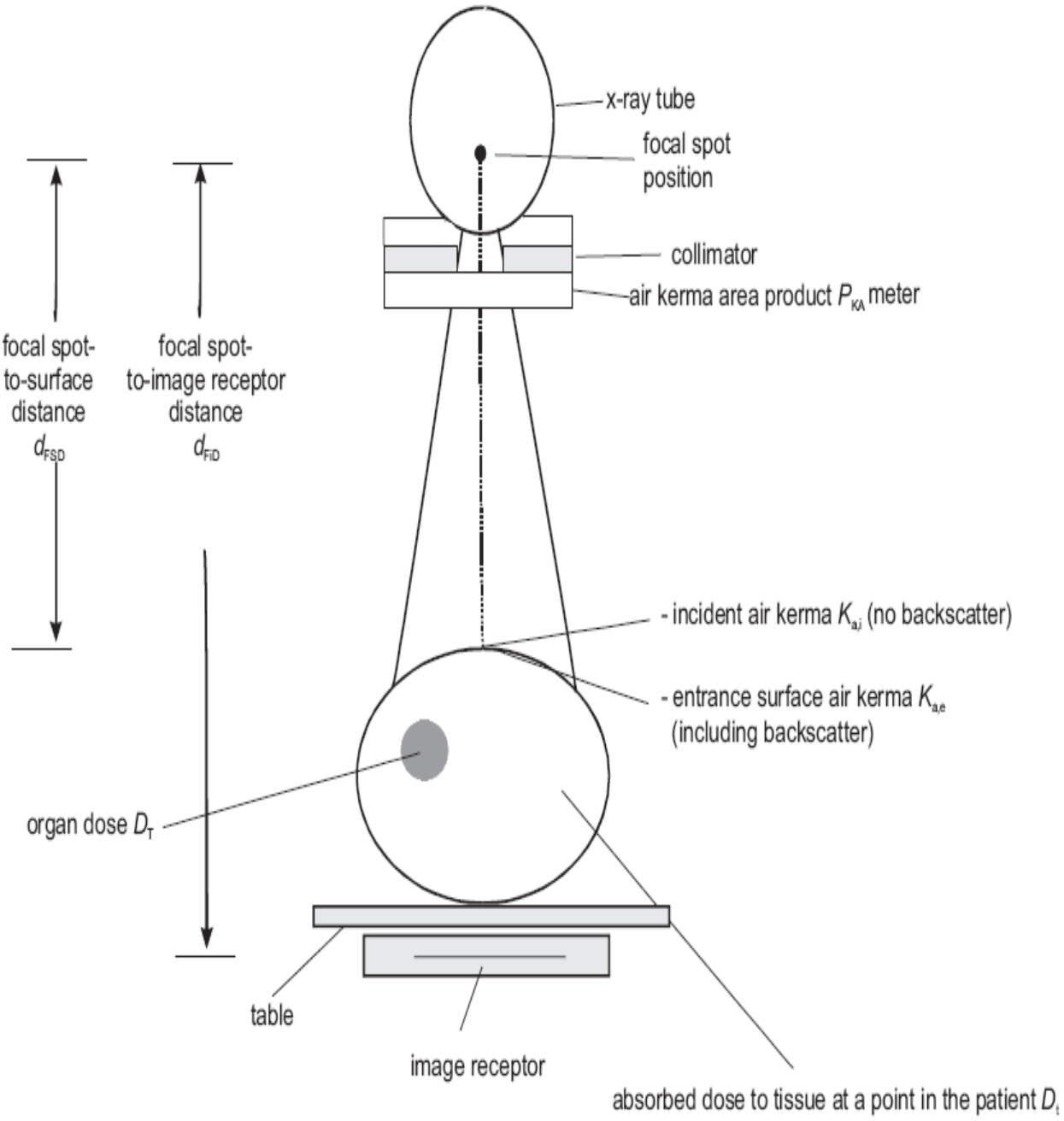

Figure (1-1). Diagram of the measuring arrangement.

1-4-6-Incident air kerma:

The incident air kerma is the air kerma from the incident beam on the central x-ray beam axis at the focal spot-to-surface distance d_{FSD}, i.e., at the skin entrance plane (Figure 1-1). Only the primary radiation incident on the patient or phantom and not the backscattered radiation, is included. We can call it as $K_{a,i}$. Unit: J/kg, special name: gray (Gy).

The incident air kerma is approximately related to the air-kerma free-in-air at any other distance, d, from the tube focal spot, K_a (d), by the inverse-square law. Thus:

$$K_{a.i} = k_a(d)\left(\frac{d}{\mathrm{d_{FSD}}}\right) \ldots\ldots\ldots\ldots\ldots\ldots\ldots\ldots\ldots (1-6)$$

It is stated approximately because there are several small corrections due to attenuation in air, scatter in air, and x-ray source structures. The incident air kerma can be easily calculated from the x-ray tube output, Y (d), provided the d_{FSD} and the tube-current exposure–time product are known for the specified radiation quality [13].

1-4-7-The incident air kerma rate ќ $_{a.i}$:

The incident air kerma rate(**ќ** $_{a.i}$) is the quotient of $dK_{a,i}$ by dt, where $dK_{a,i}$ is the increment of incident air kerma in the time interval dt, thus :

$$ќ_{\mathrm{a.i}} = \frac{\mathrm{dk_{a.i}}}{\mathrm{dt}} \ldots\ldots\ldots\ldots\ldots\ldots\ldots\ldots (1-7)$$

The SI Unit is: J/(kg/s), or Gy/s[13].

1-4-8- X-ray tube output Y (d):

X-ray tube output Y (d)) is defined as the quotient of the air kerma at specified distant d from the x-ray tube focus by the tube current-exposure time product Pit thus:

$$Y\,(d) \;=\; K\,(d) \,/\, P_{It} \;\ldots\ldots\ldots\ldots (1\text{ - }8)$$

The SI Unit is J/kg.C , if the specific name gray is used, the unit of x-ray output is Gy/C or Gy/A.S. The tube current –exposure time product, P_{It} is also referred to as the tube loading [13].

1-4-9-Entrance-surface air kerma and entrance-surface air kerma rate:

The entrance-surface air kerma is the air kerma on the central x-ray beam axis at the point where the x-ray beam enters the patient or phantom. The contribution of backscattered radiation is included. We can call it as $K_{a,e}$. Unit: J/kg, special name: gray (Gy). The entrance-surface air kerma is related to the incident air kerma by the backscatter factor, B. Thus:

$$k_{a,e} = k_{a,e}B \dots\dots\dots\dots\dots\dots\dots (1-9)$$

The backscatter factor depends on the x-ray spectrum, the x-ray field size, and the thickness and composition of the patient or phantom.

The entrance-surface air-kerma rate, ќ $_{a.e}$, is the quotient of $dK_{a,e}$ by dt, where dKa,e is the increment of entrance surface air kerma in the time interval dt, thus :

$$k_{a,e} = \frac{dk_{a,e}}{dt} \dots\dots\dots\dots\dots\dots\dots\dots (1-10)$$

The SI Unit is: J/(kg/s), or Gy/s[13].

1-4-10- Air kerma–area product and air kerma–area product rate:

The air kerma–area product is the integral of the air kerma free-in-air over the area A of the x-ray beam in a plane perpendicular to the beam axis. We can call it as P_{KA}. Thus:

$$P_{KA} = \int a\ K_{\ a}(A)dA \dots\dots\dots\dots\dots\dots\dots (1-11)$$

The SI Unit is: J m^2/kg/, or Gy m^2

If the air kerma free-in-air $K_a(A)$ is constant over the beam area, which is approximately valid for small beam areas, then:

$$P_{KA} = K_a A \dots\dots\dots\dots\dots\dots\dots\dots\dots\dots (1-12)$$

The P_{KA} has the useful property of being approximately(when air attenuation and scatter and extra focal irradiation can be neglected) invariant with distance from the x-ray tube focal spot, as long as the plane of measurement or calculation is not so close to the patient or phantom as to receive a significant contribution from backscattered radiation. Usually, the position of the plane does not need to be specified.

The air kerma–area product rate, $Þ_{KA}$ is the quotient of dP_{KA} by dt, where dP_{KA} is the increment of the air kerma–area product in the time interval dt, thus:

$$Þ_{KA} = \frac{dP_{KA}}{dt} \dots\dots\dots\dots\dots\dots\dots\dots (1-13)$$

The SI Unit is: $Jm^2/(kg\ s)$, or $Gy\ m^2/s$[13].

1-5-Quality assurance and quality control programs:

A Quality Assurance (QA) program, which includes quality control tests, helps to ensure that high quality diagnostic images are consistently produced while minimizing radiation exposure.

The QA program covers the entire x-ray system from machine, to processor, to view box.

This program will enable the facility to recognize when parameters are out of limits, which will result in poor quality images and can increase the radiation exposure to patients. Simply performing the quality control tests is not sufficient.

When quality control test results exceed established operating parameters, appropriate corrective action must be taken immediately and documented.

This guide is intended to assist the facility in setting up their QA Program and performing the quality control tests required to maintain high quality images and reduce patient exposure.

A fluoroscopy imaging system comprises an X-ray tube and generator with an image intensifier as the image receptor.

1-6-Fluoroscopy system:

The design of a fluoroscopy imaging system varies depending on the requirements and imaging demands of various radiology examinations. Fluoroscopy systems are generally characterized by their complexity and cost. Examinations carried out with a fluoroscopy system may be complex. In addition to the image intensifier, different types of cameras following the intensifier output, as well as variety of viewing monitors are required. This may all affect the over all performance of the fluoroscopy system as a whole in terms of image quality and dose received by the patient.

Most equipment function is subject to automatic control. For example the generator factors, the aperture between the image intensifier and TV camera, and the TV camera gain may all be automatically controlled. If creation aspects of the system performance deteriorate, then the system will automatically compensate, perhaps by increasing the image intensifier input dose or dose rate. Because of the nature of automatic systems, the user may not be aware of any problem. It is for this reason that it is essential to evaluate dose and dose rates with image quality of conventional and digital fluoroscopy systems.

The X-ray tube generator should be checked before commencing any quality assurance assessment of the fluoroscopy system. It is sensible first of all to check the beam quality of the X-ray tube and generator. This is achieved with a non-invasive X-ray tube potential divider used to establish the calibration of the fluoroscopic setting. The purpose of this measurement is to establish the nominal tube potential settings corresponding to stated kVp energy. This is especially useful when assessing performance and dose rates according to the manufacture specifications. The next stage is to assess the operation of the automatic dose rate control system. Patient dose rates may be assessed as well as image intensifier entrance doses. This measurement will involve the use of phantoms to simulate patients of varying thickness. Image quality phantoms containing test piece inserts are then used to assess the fluoroscopy unit. Initially the contrast and brightness setting on the monitor must be adjusted correctly. Once correct monitor adjustment is assured, then limiting resolution, low contrast detectability, high contrast detectability threshold contrast detectability and distortion may be checked along with the video signal. When the system has other image recording capabilities, such as a 100 mm camera, it is practice to test the camera at the same time as the fluoroscopy images are being assessed [14].

Chapter two
Dosimetric and image quality measurements

2-1- Dosimetry for specific purposes:

2-1-1-Dosimetry for stochastic risk evaluation:

Dosimetry quantities able to measure the stochastic risk from body irradiation are: (a) the organ equivalent dose to selected organs and tissues, (b) effective dose. These quantities represent convenient indicators of overall exposure in the assessment of diagnostic practice and population exposure and they estimate the risks to health from the stochastic effects of radiation.
The quantities are able to compare exposures from different types of procedures, irradiation geometries and radiation type and quality [15].

2-1-2-Dosimetry for quality assurance:

Dosimetry for quality assurance is addressed to evaluate the optimization level of the radiological practice, compare performance of equipment and operator skill or compare the practice among different centers. Dose and technical factor quantities are useful indicators for fluoroscopy guided procedures: (a) fluoroscopy time and/or number of acquired images, (b) total dose-area product, dose-area product for image acquisition and dose-area product for the fluoroscopy part of the procedure. For such quantities DIMOND has explored the possibility to introduce reference levels in interventional radiology for selected and common procedures [15].

2-1-3-Dosimetry to prevent deterministic effects:

For intensive image procedures in complex interventions, the knowledge of the localized dose to skin is important to assess the potential of deterministic effects of irradiation on the skin. Such quantity, expressed in term of Maximum Entrance Surface Dose (MESD) or entrance surface dose(ESD), can be assessed with different methodologies: (a) by direct calculation, with off or on-line techniques, (b) direct measurements on the patient with point detectors (TLDs or other solid state detectors), (c) direct

measurements on the patient with large area detectors (films and TLDs array), and (d) by portal monitoring with area or point/area detectors (DAP, DAP+K)[15].

The dosimetric methods for the evaluation of stochastic effects and for the purposes of quality assurance are well defined and, usually, simple to apply. They allow obtaining comparable results among different institution. In the case of the assessment of localized skin dose, the methods are complex and difficult to apply in the routine practice. Usually they are adopted for research purposes on a reduced sample of patients and procedures. The development of on-line methods, based on calculation of skin dose distribution on the patient's skin, is in our opinion, the best solution to alert practitioners when the localized skin dose is approaching the threshold for deterministic injuries [15].

2-2-Dose measurements techniques:

2-2-1-Measurement of ESD in Interventional Radiology:

Some confusion exists in the literature with regard to the definition of ESD. That is, whether the definition should refer to absorbed dose to air or absorbed dose to tissue. The consensus definition proposed by the NRPB will be adopted. Therefore, the ESD is taken as the absorbed dose to air including backscatter at the point of incidence of the beam axis with the patient entrance surface. Many different dosimetry approaches exist for the determination of ESD in IR. The following sections describe approaches to measurement of ESD from DAP, tube output, TLD measurements and 'Slow-film dosimetry [16].

2-2-2-Measurement of ESD from DAP measurements:

Use of DAP to estimate ESD may be desirable in many cases, since many departments will not have easy access to TLD's, which are often used for this purpose. Mc Parkland has developed a method utilizing DAP for the estimation of ESD (entrance skin dose; i.e. dose to tissue at the intersection of the beam axis with the patient). It has been shown that this approach to the calculation of ESD from DAP measurements can contribute an uncertainty of up to ±40% to the measurement of ESD.

In this approach DAP measurements are used to estimate the ESD to the patient by means of estimates of the field size at the entrance surface to the patient. If the beam size is sufficiently large then the assumption may be made that the dose is approximately homogeneous across the extent of the beam

area. Therefore the dose at the centre of the beam may be estimated by dividing the DAP by the beam area at the entrance surface to the patient. This approach has been shown to be quite accurate in practice. Thus the following equation can be used to calculate the ESD from DAP measurements:

$$ESD = \left(\frac{DAP}{A}\right) * C.F * BSF \ldots\ldots\ldots\ldots\ldots\ldots\ldots\ldots (2-1)$$

where:

• BSF is the back-scatter factor appropriate for any given beam kVp, field size, and HVL.

• DAP is the Dose Area Product recorded in any given instance.

• A is the beam area recorded in any given instance.

• C.F. is the calibration factor for the DAP meter estimated using a standard.

This beam area may then be corrected geometrically to the entrance surface of the patient if either:

(a) It can be assumed that the tube focus to patient entrance surface distance, FSD, and tube focus to image intensifier entrance surface, FID, are determinable and practically the same for each projection in a certain IR procedure, or:

(b) The FSD can be determined from existing recordings of FID and patient characteristics;

The following equations may be used respectively to correct the beam area to the entrance surface with the patient in either case:

$$A(FSD) = A(FID) * \left(\frac{FSD}{FID}\right)^2 \ldots\ldots\ldots\ldots\ldots\ldots\ldots\ldots (2-2)$$

$$A(FSD) = A(FID) * \left(\frac{FID - W}{FID}\right)^2 \ldots\ldots\ldots\ldots\ldots\ldots (2-3)$$

where A (FSD) and A (FID) are the area of the beam at the entrance to the II and the entrance to the patient respectively, and W is the equivalent thickness of the patient. This equation may be used in situations involving fixed systems where the II is brought close to the exit surface with the patient to eliminate scatter. The Finnish Radiation Protection Authority (STUK) have developed regression models which describe the variation in weight with height, and corresponding variation in body thickness with such parameters. The regression function takes the following form:

$$y = ax + b \dots\dots\dots\dots\dots\dots\dots (2-4)$$

where: x is weight of the individual in kilograms, y is the width or thickness of the region concerned, a, b are the regression parameters.

This is a procedure that can be used for both mobile and fixed fluoroscopy systems [16].

2-2-3-Measurement of ESD from Tube Output Measurements:

ESD may be calculated in practice by means of knowledge of the tube output. This is useful in situations where the tube does not have a DAP facility. Tube output measurements are routinely acquired during the QC performed on X-ray equipment. In such instances, the following equation may be used:

$$ESD = O/P * \left(\frac{kVp}{80}\right)^2 * mAs * \left(\frac{100}{FSD}\right)^2 \dots\dots\dots\dots (2-5)$$

where:

• O/P is the tube output per mAs measured at a distance of 100cm from the tube focus along the beam axis at 80 kVp.

• kVp is the beam kVp recorded for any given examination (in many cases the output is measured at 80 kVp, and therefore this appears in the equation as a quotient to convert the output into an estimate of that which would be expected at the operational kVp). The value of '80' should be substituted with whatever kVp the actual output is recorded at any given instance).

• mAs is the tube milli-Amp-current-time which is used at any given instance.

• FSD is the focus to entrance surface distance used at any given instance [16].

2-2-4-Estimation of ESD from TLD measurements:

TLDs are accepted as the best standards for estimation of entrance surface dose in practice. In interventional radiology, they are commonly placed around and at the centre of the entrance surface to the patient at points where the maximum exposure is anticipated to occur. This requires knowledge of the procedure and exposure pattern that is to be employed by the clinician to be available prior to the start of the procedure. TLDs are read in the standard manner and the maximum value read is used as an estimate of the maximum ESD received by the patient. Frequently, many TLDs are spaced around the

irradiated area on both the entrance and exit site to enable the determination of the most irradiated area and maximum surface (or skin) dose. Again, there is a requirement that the location of the most irradiated area is known prior to the start of the procedure so that the number of TLDs used per patient is minimized. The advantage is that the measurement is the most accurate in-vivo estimate of skin dose available [16].

2-2-5-Estimation of ESD using Slow Films:

The method for estimation of ESD using radiotherapy slow films was developed. These films are used for the verification of patient doses and orientation in radiotherapy procedures. In IR procedures, the film is placed underneath the patient and exposed throughout the normal IR protocol. The films are calibrated by standard sensitometer, and read by densitometry. They have a linear range from 400mGy to 2000 mGy for Co^{60} energies, which makes them ideal for identifying whether deterministic levels for skin have been exceeded. When used in conjunction with DAP and TLD measurements of ESD, it is found that the measurements were within 5%-20%. The films can be used to estimate total ESD, total DAP, or maximum ESD [16].

2-2-6-Radiochromic media:

Radiochromic dosimetry media (commonly referred to as “films”) can be handled in normal lighting conditions, are self-developing, respond nearly immediately to exposure to radiation, and they require no chemical processing. They are used to measure absorbed dose and to map radiation fields produced by X-ray beams in a manner similar to that of portal film. As such, radiochromic media have the same advantage of locally specific dose monitoring without error resulting from beam reorientation or backscatter. And radiochromic film can be examined during a procedure if there is a need to obtain an estimate of skin dose. Exposure to ionizing radiation causes radiochromic film to immediately change color and darken. The degree of darkening is proportional to exposure and can be quantitatively measured with a reflectance densitometer. There does exist a gradual darkening of the film with time and darkening is usually maximum within 24 hours. However, the amount of darkening within the period immediately following the initial exposure is not large and does not interfere with the ability to use it for skin dose guidance during a procedure as long as this phenomena is understood and taken into account.

A limited quantity of radiochromic films was distributed to the centers to be used nearly exclusively for cardiac examinations. Some centers had their own films and used them for additional studies. For cardiac work, films were placed on the table under the patient pad in such a way that the most heavily exposed parts of the body were covered by the film. Necessary data, such as the beam orientation (superior, inferior etc.), patient ID, date, and type of examination, were recorded on the film.

When used in the manner described, the film darkening includes backscatter, and beam reorientation and field non-uniformities are recorded. The only correction factor necessary is the conversion from entrance air kerma at the skin to absorbed dose in the skin. Merely multiplying the recorded entrance air kerma at the skin by an f (E) of 1.06 renders estimated absorbed skin dose [17].

2-2-7-mesurement of effective dose (E) in interventional radiology:

Effective Dose (E) has been introduced as an estimator of the potential for detriment from exposures to ionizing radiation. Recently many reports have been written on methods for the estimation of (E) in Interventional Radiology. Various techniques have been employed which depend on procedure type, methods of estimation of conversion coefficients, and quantity to be used as an estimator for (E). In IR, coefficients for the estimation of (E) from DAP and ESD measurements have been developed. They have been calculated from Rando phantom measurements and Monte Carlo simulations on photon transport in mathematical phantoms. However, given that the fluoroscopy and radiography sequences may vary significantly throughout a given procedure, it is difficult to characterize an IR procedure for the purposes of calculation of (E). Consequently approaches to the calculation of (E) vary widely in accuracy, where some employ a single conversion coefficient for the procedure as a whole, while others calculate conversion factors which are specific to each radiography and fluoroscopy projection throughout the procedure. Further still, automated systems which allow the calculation of (E) from any number of defined exposure projections and conditions have been developed.

Indeed, there is a significant uncertainty in any calculation of (E) where deviations in exposure factors, irradiation geometry and patient characteristics (from those for which the conversion factors have been calculated) invariably exists. In many cases the size of this uncertainty is not known, but is thought to have a minimal value of a factor of 2 surrounding the estimate. Consequently, (E) has significance as a normalization of the detriment attributable to exposures of different individuals in IR, but the

uncertainty in its calculation leads to the conclusion that DAP is a more appropriate estimator of the stochastic detriment from exposures in IR[16].

2-3-Image quality measurements:

Image quality measurements are needed for several purposes, such as equipment design, performance specification, acceptance and constancy testing in quality assurance and imaging technique optimization. Most commonly the evaluation of image quality is based on a subjective assessment, either from the images of actual patients or from those of suitable test phantoms. In addition to these methods, there exist several objective measures that can be used to achieve more precise and portable results.

2-3-1-Visual evaluation methods:

In medical imaging it is necessary to define image quality with respect to what is needed to be detected in the image, i.e. as a task-based quantity. Therefore, it may be thought that the most useful way of measuring image quality would be using actual patient images and radiologists. In principle, diagnostic performance can be measured using the receiver operating characteristic (ROC) methodology, but in practice this is too laborious for routine evaluation purposes. Clinical image quality criteria that are based on the visibility of normal anatomy which have been suggested for quality assurance use and imaging technique optimization tasks. Of course, both approaches are important and useful for many purposes, but it is difficult to see how either of them could be considered as an actual measurement that can be calibrated, repeated and compared with results obtained elsewhere. In addition to image quality, the results depend on the patient material and the radiologist interpreting the images. In the case of clinical quality criteria, the actual significance of the criteria for diagnostic performance is not always guaranteed and the subjective nature of the evaluation will cause additional variability in the results. It cannot be expected that other than exceptionally large changes in imaging performance will be reliably noted by this method.

The imprecision caused by the variability in patients can be avoided by using test phantoms instead of patients. This would improve the sensitivity and precision of the assessment and allow, at least partly, the test to be repeated by others. Phantoms can be manufactured with a variable amount of anatomical detail, but usually simple homogeneous phantoms that mimic the radiation attenuation and scattering

properties of the human body will suffice. Common test details consist of disks of various contrasts and diameters for measuring the low-contrast-detail detectability (contrast resolution) or contrast-detail performance or lead bar patterns for measuring the limiting spatial resolution. The latter are most often used without an attenuating phantom in order to measure the maximum spatial resolution of the imaging system. In these tests, a numerical test result is obtained, which expresses the faintest or smallest detail seen in the image [18].

2-3-2-Objective measurement methods:

In addition to the visual measurements, there exist objective measures related to large-area signal transfer (K), image sharpness (MTF) and image noise (NPS). These can be combined to form the quantity NEQ:

$$NEQ\left(\int x, \int y\right) = \frac{K^2 * MTF^2\left(\int x, \int y\right)}{NPS\left(\int x, \int y\right)} \dots\dots\dots\dots\dots\dots\dots\dots\dots\dots\dots\dots (2-6)$$

which can be interpreted to express the quantum fluency that the image is worth at various spatial frequencies (fx, fy). NEQ can be compared with the actual fluency at the image receptor (Q). This results in the DQE:

$$DQE\left(\int x, \int y\right) = \frac{NEQ\left(\int x, \int y\right)}{Q} \dots\dots\dots\dots\dots\dots\dots\dots\dots\dots\dots\dots (2-7)$$

which expresses the efficiency with which the imaging system uses the information carried by the quanta impinging on it.

DQE measures the efficiency of the image receptor, it does not refer to the patient's dose and neither NEQ nor DQE take into account all factors that influence the detectability of the actual object detail, such as the energy dependence of the radiation contrast. These image quality descriptors are therefore not sufficient when, e.g. the imaging conditions are being optimized. They are intended for the evaluation of only one component of the imaging system: the image receptor. If the noise in the image is normally distributed and signal-independent, and the imaging system is linear and shift-invariant, the best possible observer can detect a detail object (DS(fx, fy)) with the SNR:

$$SNR^2 = [\int (K^2 * MTF^2 \left(\int x, \int y\right) * \Delta S \left(\int x, \int y\right)^2) / NPS \left(\int x, \int y\right)] d \int x \, d \int y$$

$$= \frac{[\Delta I(\int x, \int y)^2]}{[NPS(\int x, \int y)] d \int x \, d \int y} \ldots\ldots\ldots\ldots\ldots\ldots\ldots (2-8)$$

where the expected (noiseless) image of the detail has been denoted by ΔI (fx, fy). This SNR specifies the ideal observer's detection performance of the given detail completely. For example, the fraction of correct answers the ideal observer achieves in multiple alternative forced-choice (MAFC) tests or its whole ROC curve can be calculated from this quantity. The ideal observer's SNR is the proper quantity to use when the task-dependent image quality is considered; it takes into account all factors of importance, including the subject contrast. If it is required to relate image quality to the patient's dose, one can evaluate the dose efficiency by calculating the quotient SNR^2/D, where D is the patient dose and can be either the entrance dose or the effective dose, whichever is more appropriate for the evaluation. Image quality measurement in fluoroscopy differs only slightly from the above discussion of static images. However, in this case the NPS and MTF are 3-D quantities: in addition to the two spatial frequencies, they also depend on the temporal frequency.

The measurement of the spatial-temporal NPS is straightforward but we are aware of no practical methods for the direct measurement of the spatial-temporal MTF. However, in most imaging systems it may be possible to assume it to be of form:

$$MTF\left(\int x, \int y, \int t\right) = MTF(\left(\int x, \int y,\right) MTF(\int t) \ldots\ldots (2-9)$$

The SNR^2 of static imaging must be replaced by the accumulation rate of SNR^2, which we denote as SNR^2 rate. It describes the accumulation of information with the temporal length of the image sequence. At first thought, it would appear that the measurement of SNR^2 rate in fluoroscopy would be much more complicated than the measurement of SNR in static imaging. It is, in fact, the other way round. Measurement in fluoroscopy is very easy because a large number of image samples can be readily obtained. The measurement can be done either by analytical calculation, using equation (of SNR^2) applied to temporal averages of image sequences of reasonable lengths, or by constructing a quasi-ideal observer and letting it observe image samples[18].

Chapter three

Materials and methods:

Quality control measurements were performed for six digital fluoroscopy units. Materials and methods used in this study are summarized in this chapter.

Technical parameters units are present in Table 3-1:

Table (3-1): Technical information for the fluoroscopy units

Hospital name	**Configuration**	**Manufacturer**	**Generator: mode, year**	**Tube: model, year**
Ibn Cena (ISH)	C-arm	DORNIER	COMPULS	DF-1515B-T
Ahmed Gasim1 (AGH1)	C-arm	TOSHIBA	CAS-10A, Des 2000	DRX-T7445GDS Nov2000
Ahmed Gasim2 (AGH2)	C-arm	ALLENGERLIFE, VARIAN		B160H Jan2007
Alshab (ASH)	C-arm	SHIMADZO	II model: TH9438	
Alneelen Center (ANC)	C-arm	SIMENS	1170427X2169	1184696
Open Heart Hospital (OHH)	C-arm	PHILIPS		1998

3-1-Dose measurement instruments and phantoms:

In the present study, entrance surface air kerma ESAK rate, kVp, HVL and image intensifier input air kerma rate measurements were performed by using (Piranha) multimeter device (RTI Electronics AB, Göteborgsvägen 97/50, SE-431 37 Mölndal, Sweden). The (Piranha) was designed as a truly "self-contained", all-in-one, multi-function meter that fits in the palm of your hand. The standard detectors are built-in. Communication is made very easy by built-in Bluetooth and USB. With its long-life battery you can count on it to last even during the busiest day. It is small and light enough to slip into your shirt pocket, and comes with a compact carrying case. The Piranha can do it all in one shot; kV, time, dose, dose rate, HVL, and total filtration. With pulsed fluoroscopy you add pulse rate and dose/pulse. It measures on Cine and Dental, panoramic and Intra-Oral, as well as traditional and slot scanning mammography. There is even a Piranha that measures CT dose profiles. The Piranha assures accurate results in a simple, fast, and smart way. Also Piranha can measure image intensifier input dose rate by linking it with small external ion chamber.

To simulate patient size in different thicknesses polymethylimethacrylate (PMMA) material phantom was used which was made of patient tissue equivalent matter.

3-2-Image quality measurement instruments:

For assessment of image quality, Huttner Type 53 line pair phantom has been used for measurement of the spatial resolution. The contrast detail phantom (TO10) was used for determination of contrast detail performance.

3-3-Materials and methods:

3-3-1-Visual check:

All foot and hand switches designed to energize the fluoroscopic tube were tested to ensure that x-ray production is terminated as soon as the switch is released. In case switches have multiple positions (e.g. high level control) each position was be tested including: table, image intensifier, grid movement (in , out), Bucky movement , lead drapes fixation around the tube and x-ray tube, to check smoothly and freely without requiring excessive force.

3-3-2- Tube voltage accuracy:

Any users added or adjusted filtration in the x-ray beam was removed or set to the minimum value before proceeding with the test if possible. The lead rubber sheet or PMMA thickness was placed on the face of image intensifier to protect the input phosphor from the unattenuated primary x-ray beam. Piranha multimeter was placed between the x-ray tube and the image receptor so that it faces the beam focus. The measurement was done with standard focus-image intensifier distance of 1 meter and fluoroscopic system operated at its normal operation conditions. A series of measurements were obtained at a constant tube current (e.g. 1 mA) commencing with lowest available tube voltage (kVp) and increasing in about 10 kVp steps until maximum available tube voltage was reached. In case manual control of the fluoroscopic exposure factors is not available, a range of attenuators was used like PMMA thickness at the image intensifier input to obtain different tube voltage (kVp) values [2].

3-3-3- Beam Quality (HVL):

Any users added or adjusted filtration in the x-ray beam was removed or set to the minimum value just like the normally used, then any PMMA thickness was placed between the tube and image intensifier to induce the radiation in any kVp value. Piranha multimeter was placed between the tube and image intensifier and taking HVL value from one exposure or more HVL values.

3-3-4- Automatic Exposure Control:

Different thicknesses of PMMA were used to simulate the patient on patient Table. In each PMMA thickness the entrance surface air kerma rate was measured at the image intensifier input face by using external ion chamber attached with (Piranha) to get a reading. Then deviations between kerma rate readings were calculated.

3-3-5- X-ray field limitation and minimum source-to-skin distance:

The distance between the X-ray tube and the image intensifier was adjusted to the maximum, the largest image intensifier field of view selected and fully open collimator. Plate of lead numbers was used which was placed on the face of image intensifier to see the lead numbers on the TV monitor and determine the limit of fields after taking exposure.

The table of the patient was moved to the minimum distance to focal spot position and this distance was measured by using tape meter. This distance will actually be focal to skin distance.

3-3- 6-Threshold contrast detail detectability:

The common clinical mode of operation was used. i.e. pulse rate, dose level, total filtration, …etc. The phantom (TO10) was placed at the centre of the x-ray field close to the image receptor entrance plane. The fluoroscopy unit was operated with AEC. 2 mm Cu placed close to the X-ray tube face. The images were acquired as the soft copy on TV monitor. The image of the phantom was examined by several observers (radiologist, physicists) and evaluated at threshold level visibility as seen by the gropes of the (TO10) phantom. The TCDD curve was plotted on log-log scale between threshold detection index (HT) as a function of the square root of the detail area $\sqrt{}$ (A), thus:

$$HT(A) = \frac{1}{CT * \sqrt{A}} \dots\dots\dots\dots\dots\dots . (1-3)$$

where CT is threshold contrast (%), given by the manual of the object test (TO10). Then the assessment of contrast can be easy by seeing to the curve and evaluating the result obtained.

3-3-7- Limiting Resolution:

Huettner type 53 resolution grid test object was placed at the centre of the field, mounted directly on the image intensifier input surface oriented at 45 degree to the television raster lines. A low kVp (40-60) with low filter was used (0.5 cm of PMMA) to achieve the highest possible contrast and make an exposure to obtain image of test object as a soft copy on TV monitor for all field sizes available. Resolution of all field sizes was determined.

3-3-8- Patient entrance surface air kerma ESAK rate under automatic exposure control:

The distance between the x-ray tube and the image intensifier was adjusted at about 1 meter. The radiation detector (Piranha) was placed on the table before the attenuating material (PMMA) to simulate the patient and the AEC operation mode was started. Then the entrance surface air kerma rate measurements were taken with different modes of operation, field size and (PMMA) thicknesses.

3-3-9- Image intensifier input dose rate under automatic exposure control:

1m distance between the tube and image intensifier was taken, different thicknesses of (PMMA) were placed on the face of the tube, and in case of no way, 2mm of Cu was used. Small ionization chamber was attached to the image intensifier face which was connected with (Piranha). The measurements were taken for all field sizes and modes under automatic exposure control.

3-3-10-Radiation protection devices for occupational exposure:

To the radiation protection to patients and staff were observed and recorded. The radiation protection devices included the lead equivalent aprons, gloves, thyroid shield, ceiling mounted lead glass screens.

Chapter four

Results and Discussion:

4-1-Results:

In this study measurements have been made for the quality control of six digital fluoroscopy units. Table 4-1 presents results of the measurements made for various kVp and HVL values. kVp values generally fall within the international recommended limits. All units were C-arm configuration.

Table (4-1). Results for various peak tube voltage and half-value layer values.

Hospital	kVp set	kVp measured	kVp Accuracy%	HVL / mm	Minimum HVL required mm	Unit use
ISH	85	97.8	15.1			IR
	63	63.8	1.3			
	86	78.0	9.3			
	90	76.0	15.6	3	3.2	
	72	70.0	2.8			
	61	74.0	21.3			
AGH1	95	88.9	6.4			Cardiology
	53	77.4	46.2	3.0	1.9	
	84	94.7	12.8	5.3	3.0	
	97	105.5	8.8	5.9	3.5	
	123	117.9	4.1	6.6	4.5	
AGH2	125	122.5	2	5.5	4.5	Cardiology
	107	105.0	1.9	4.7	3.8	
	89	90.4	1.6	3.9	3.2	
	96	99.0	3.1	4.5	3.4	
	76	78.0	2.6	3.5	2.7	
	66	67.0	1.5	3.9	2.3	
	71	73.0	2.8	4	2.5	
ASH	68	65.5	3.7	4.1	2.5	Cardiology
	77	80.3	4.3	5.1	2.8	
	82	83.8	2.3	5.2	3.0	
	92	90.9	1.2	5.5	3.3	
	102	102.6	0.6	6.1	3.6	
	111	115.8	4.3	7.0	3.9	
ANC	110	110.4	0.4	4.5	3.9	IR
	106	107.0	0.9	4.3	3.7	
	83	87.3	5.1	3.2	3.0	
	63	68.0	7.9	2.4	2.3	
OHH						Cardiology
	66	66.45	0.7	2.8	2.4	
	72	72.83	1.2	3.1	2.6	
	91	89.34	1.8	3.7	3.2	
	96	95.74	0.3	4.0	3.4	
	104	104.4	0.4	4.4	3.7	
	110	110.0	0.0	4.7	3.9	

Entrance surface air kerma rate ESAK rate was measured using (Piranha). Table 4-2 shows the measurements of ESAK rate for six fluoroscopy units. The ESAK rate is within the established international references dose levels with exception to few cases when fluoroscopy unites were operated in cine mode.

Table (4-2). Entrance surface air kerma ESAK rate.

Hospital	PMMA thickness cm	Field of view cm	mode	ESAK mGy/ min	Unit use
ISH	18		Floro pulsed	21.3	IR
				22.1	
				23.4	
			Floro continuous	30.9	
				41.3	
				64.8	
AGH1	22	23	Pulsed	30.7	Cardiology
		18		20.4	
		12		6.8	
	20	23		6.1	
		18		10.8	
		12		21.7	
	18.5	23		8.8	
		18		9.6	
		12		13.3	
	16.5	23		8.3	
		18		8.4	
		12		9.4	
	16	23	Cine	11.5	
		18		741.6	
		12		956.4	
	18.5	12		840.0	
	22	12		744.0	
AGH2	18.5	12	Floro 25pps	52.6	Cardiology
		16		34.9	
		22		16.9	
		12	Cine 12pps		
		16		264.5	
		22		177.2	
	20	12	Floro 25pps	177.2	
		16		59.9	
		22		38.9	
		12	Cine 12pps	342.0	
		16		250.2	

		22		191.8	
	22	12	Floro 25pps	73.2	
		16		94.6	
		22		51.1	
		12	Cine 12pps	390.0	
		16		127.8	
		22		336.3	
ASH	20	19	Floro 30pps	40.1	Cardiology
		15		49.1	
		12		57.5	
		19	Floro 15pps	31.3	
		15		37.9	
		12		51.1	
		19	Floro 7.5pps	10.8	
		15		10.9	
		12		10.7	
		19	Floro continuous	36.5	
		15		34.5	
		12		52.6	
		19	Cine 30pps		
		12	Cine 15pps	12.9	
		15	Cine 15pps	7.7	
		15	Cine 7.5pps	7.3	
		15	Cine 30pps	8.7	
***ANC**	22	21	Floro continuous	31.6	IR
		21		35.1	
		21*7		34.4	
		7		33.7	
	20	21		34.8	
		21*7		34.4	
		7		33.4	
	18.5	21		34.8	
		21*7		34.2	
		7		33.3	
OHH	22	23	Normal	45.1	Cardiology
		17		49.6	
		14		56.2	
		23	High	64.0	
		17		75.5	
		14		96.8	
	20	23	normal	40.5	
		17		50.1	
		14		47.1	
		23	high	59.9	

	17	73.0
	14	76.1

*In (ANC) field sizes were: 21*21cm^2 circle, 21*7cm^2 rectangular, and 7*7cm^2 square.

Table 4-3 shows image intensifier input air kerma rate. These results are high compared to international recommendations. The results could be attributed to the use of grid with unknown grid factors.

Table (4-3). Image intensifier input air kerma rate.

Hospital	**PMMA Thickness cm**	**Field of view cm**	**mode**	**Image intensifier input air kerma rate µGy/s**
ISH	18.5	Small	Floro continuous	1.9
		Medium		1.5
		Large		1.6
AGH1	22	12	Floro Pulse	41.1
	20			56.2
	18.5			70.4
	16			80.6
AGH2	22	12	Floro 25pps	10.9
	20			13.5
	18.5			16.9
ASH	20	19	Floro 30 pps	9.8
			Floro 15pps	1.7
			Floro7.5pps	0.7
			Floro continuous	2.6
ANC	6	21*7	Floro continuous	5.2
		7		5.3
		21		5.2
	12	21		4.8
	17			3.9
	20			3.9

Image quality measurements in terms of limiting resolution were done by using (Hettner type 53 phantom test pattern). Table 4-4 shows the limiting resolution measurements in Lp/mm. The measurements were obtained for all systems and the measured resolution was well within recommended values.

Table (4-4). Limiting resolution results.

Hospital	Field of view cm	Image intensifier diameter cm	Resolution Lp/mm
ISH	Between 19 to 22	23	2.0
AGH1	23	26	2.2
AGH2	22	23	2.2
ASH	18.8	23	1.8
ANC	21	23	1.2
	21*7		1.2
	7		1.2
OHH	23	26	1.6
	17		1.4
	14		1.0

Table 4-5 shows the field size limitation and source to skin distance which were for all systems well within recommendations. The measurement of field limitation was done by using conceding test tool of radiography (square plate with pb numbers) by putting it in patient position and calculating the magnification and finding the actual field size in image intensifier.

Table (4-5). Field size limitation and minimum source to skin distance.

Hospital	Image intensifier diameter cm	Maximum field of view measured cm	Minimum source to skin distance measured cm
ISH	23		65
AGH1	26	23.0	70
AGH2	23	22.3	56
ASH	23	18.7	
ANC	23	21.0	65
OHH	26	23.0	49

Automatic exposure control was checked for three fluoroscopy units. Table 4-6 shows the air kerma rate at the image intensifier input surface.

Table (4-6). Image intensifier input air kerma rate for different PMMA thicknesses at three hospitals.

Hospital	Thickness cm	Mode	Image intensifier input air kerma rate µGy/s	Standard deviation%
AGH1	18.5	Floro 25pps	16.6	5.9
	20		17.6	0.0
	22		18.7	6.0
ANC	6	Floro continuous	5.2	17.5
	12		4.8	7.6
	17		3.9	12.1
	20		3.9	12.8
OHH	6	Normal	9.7	
	12		5.2	18.1
	17		6.2	2.4
	20		6.9	8.7
	22		7.1	11.8

Radiation protection in all units were in terms of lead apron. The aprons had thicknesses above of 0.25 mm lead which is as recommended. Protection In terms of gloves, screens and thyroid protection were neglected in most units. Table 4- 7 shows the result of the survey.

Table (4-7). Radiation protection devices survey.

Hospital	Aprons No	Pb (mm) equivalent	Thyroid protective device	Gloves No	Protective screens
ISH	5	0.5	2	No	No
AGH1	13	0.5	2	No	No
AGHS	13	0.5	2	No	No
ASH	8	0.35	No	No	No
ANC	2	0.5	No	No	No
OHH	9	0.5	No	No	No

Figures (4-1), (4-2),(4-3),(4- 4),(4- 5), and (4-6) show the image quality curves in terms of threshold contrast detail detectability TCDD which were done by using TO10 contrast test tool for all systems. The curves were plotted between threshold detection index Vs square root detail area.

Figure 4-7 presents the comparison between the threshold contrast detectability curves for the systems. The results show good agreement.

Note: in the figures 4-1, 4-2, 4-3, 4-4, 4-5, 4-6 and 4-7 field size refers to field of view.

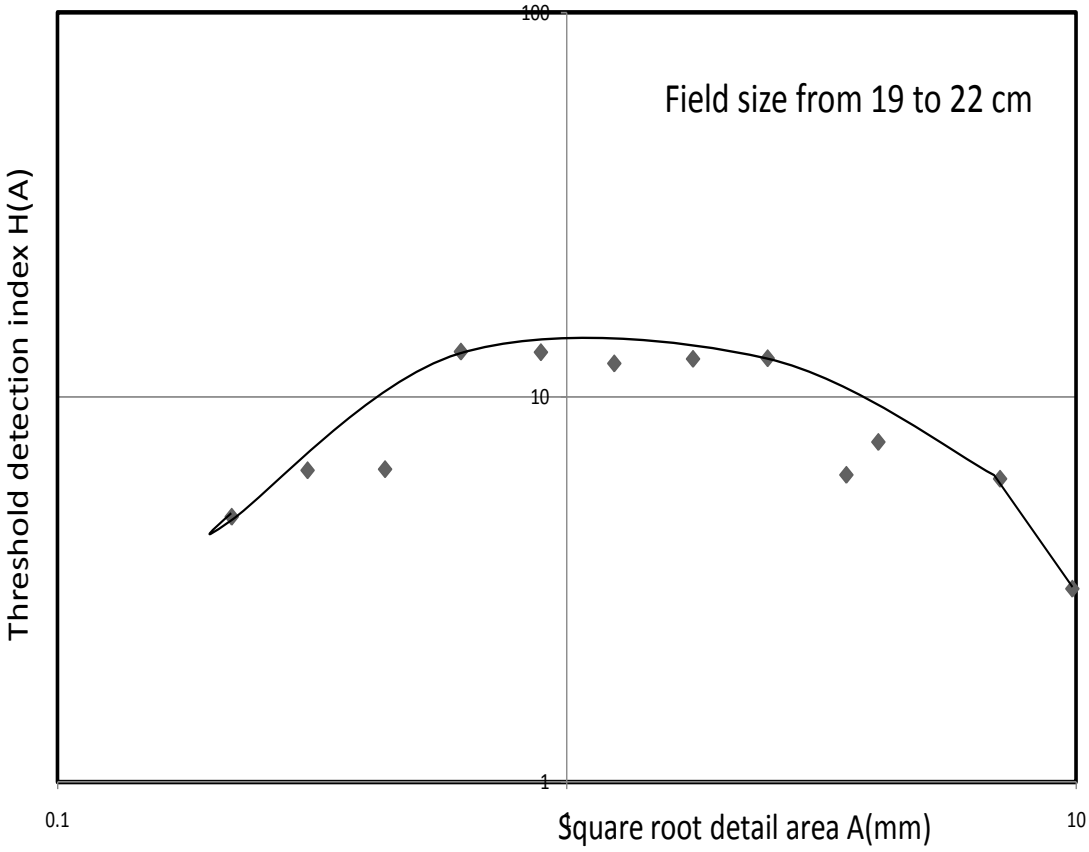

Figure (4-1). Threshold contrast detail detectability curve for (ISH) fluoroscopy unit.

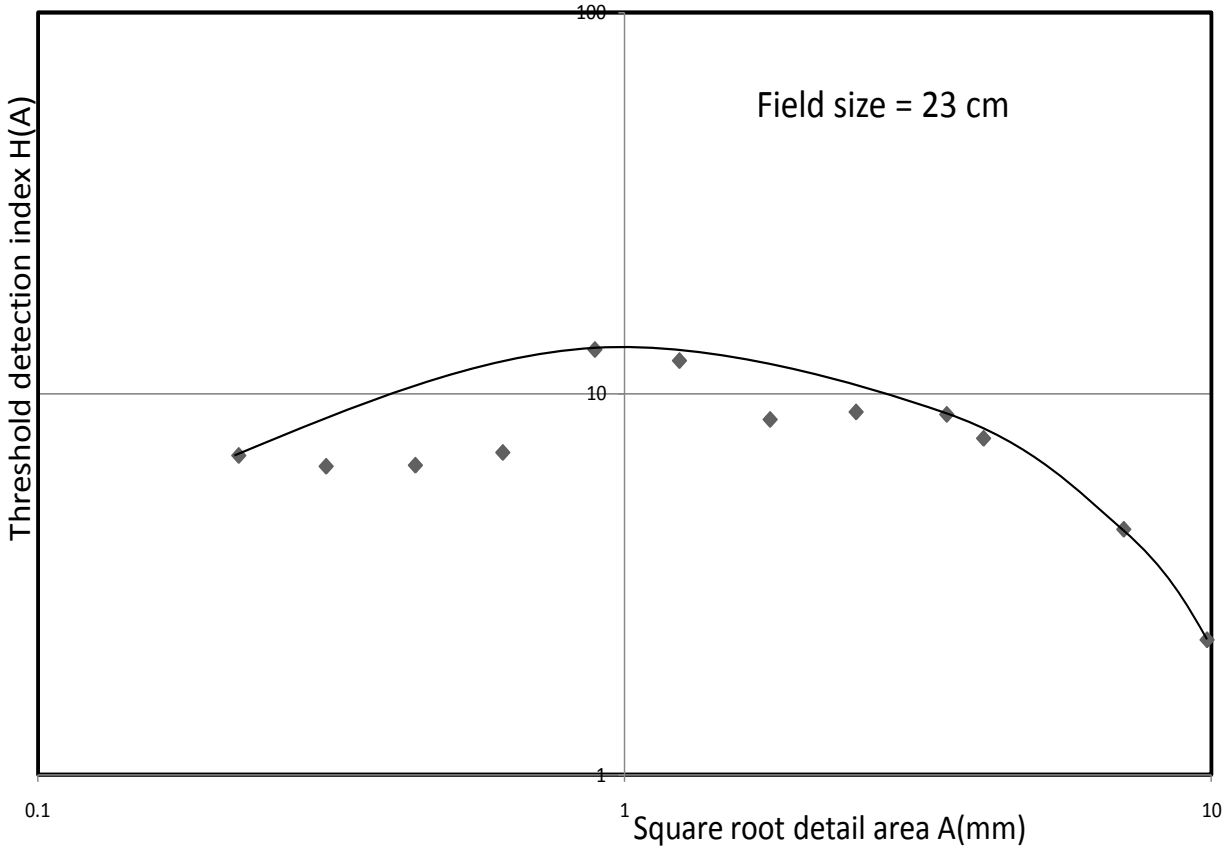

Figure (4-2). Threshold contrast detail detectability curve for (AGH1) fluoroscopy unit.

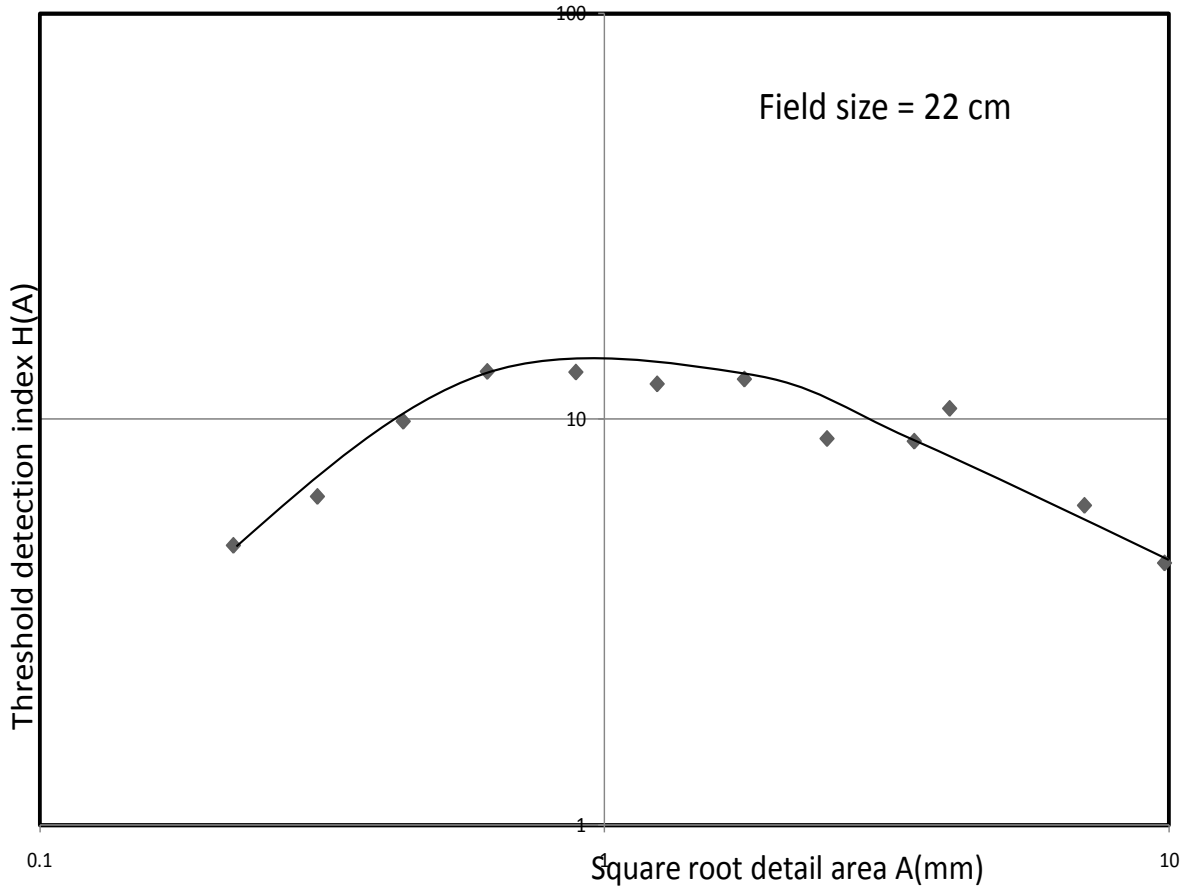

Figure (4-3). Threshold contrast detail detectability curve for (AGH2) fluoroscopy unit.

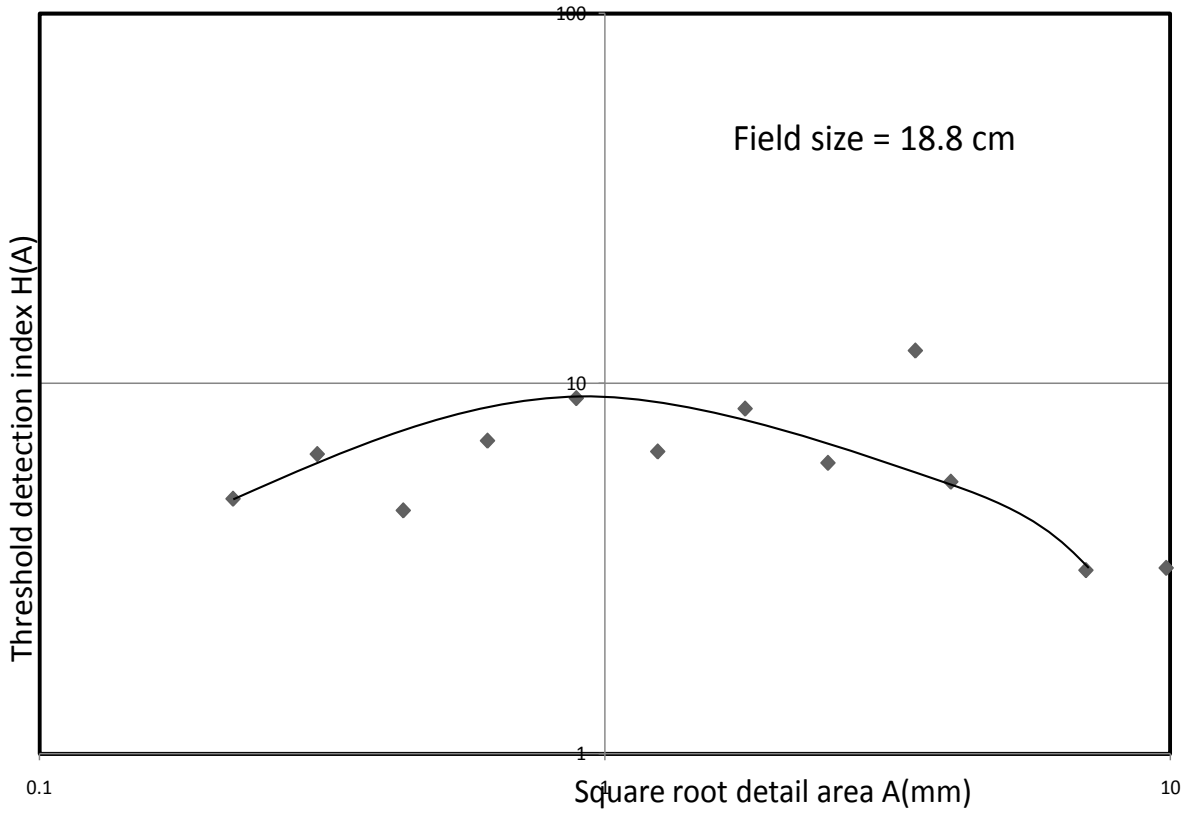

Figure (4-4). Threshold contrast detail detectability curve for (ASH) fluoroscopy unit.

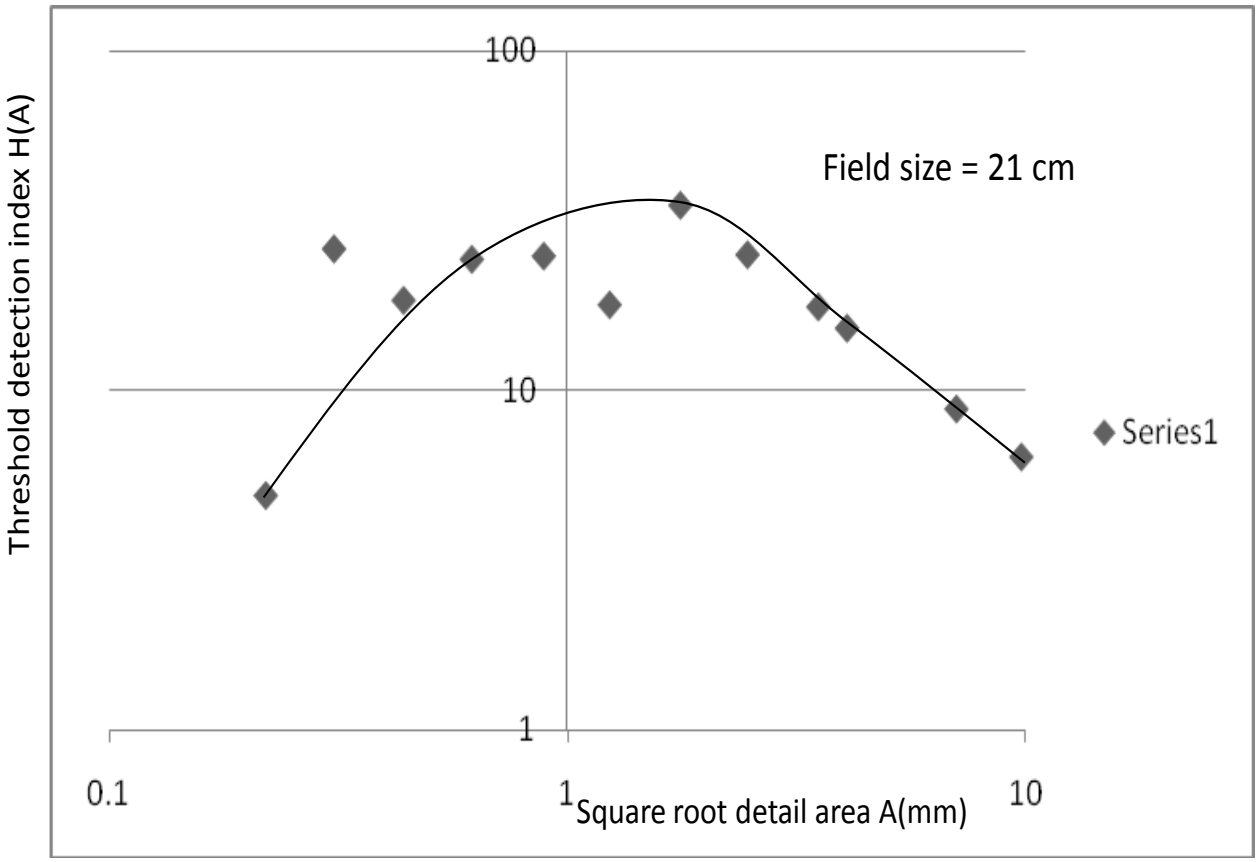

Figure (4-5). Threshold contrast detail detectability curve for (ANC) fluoroscopy unit.

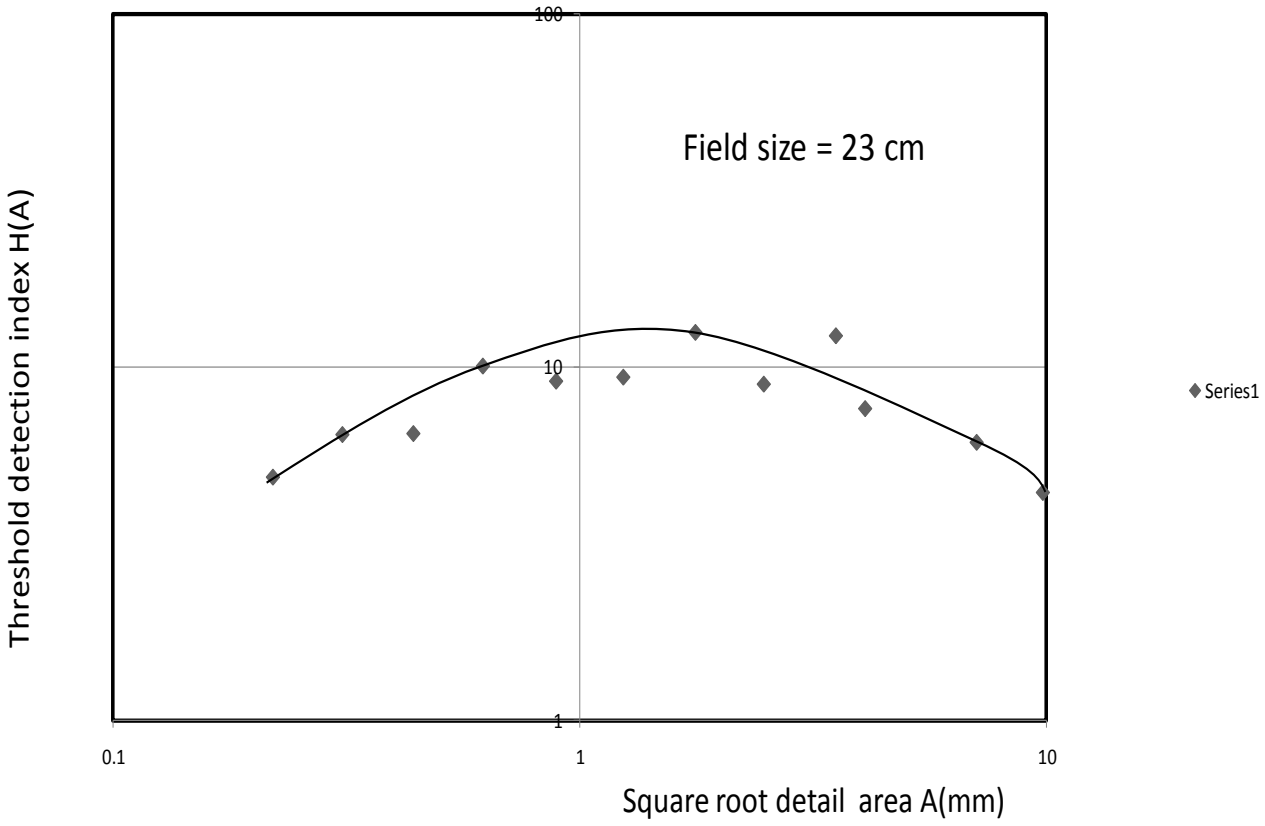

Figure (4-6). Threshold contrast detail detectability curve for (OHH) fluoroscopy unit.

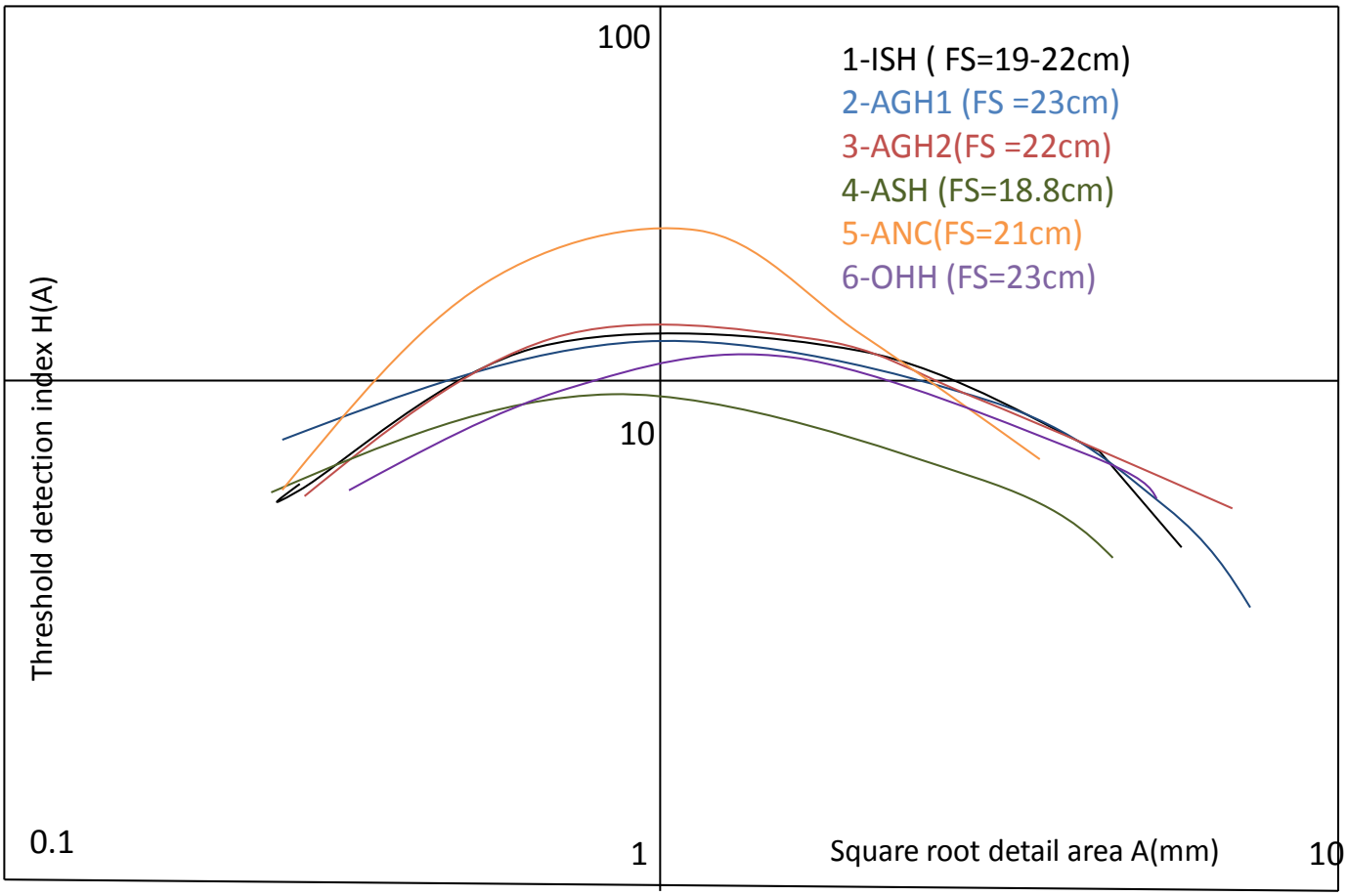

Figure (4-7). Threshold contrast detail detectability curves for six fluoroscopy units.

4-2-Discussion:

4-2-1-kVp and HVL accuracy:

As show in Table 4-1, the kVp accuracy was not as proposed in international recommendations i.e. ≤ 10% [2]. This is evident in (ISH) and (AGH1) where the deviation was about 21% and 19%, respectively.

As presented in Table 4-1, the HVL was above the minimum value recommended in Ref.[19]. The measured values of HVL and kVp were similar in all fluoroscopy units.

The measurements were compared to results of Ref. [3]. The kVp deviation in this study was larger than the deviation reported in Ref. [3], except for fluoroscopy unit in hospital (OHH).

HVL measured in this study was better than that reported in Ref. [3]. This is not surprising since different fluoroscopy units might be using different amount of filtration.

4-2-2-Image intensifier input dose rate:

All fluoroscopy systems were with fixed grid. The doses were high and exceeded the recommended levels as shown in Table 4-3 by using different thicknesses of PMMA phantom and field sizes.

The calculation of dose was done without the knowledge of grids transmission factors.

All measurements of image intensifier input dose rate must be done with grid removed or knowing the transmission factors of grid used and compared to the recommended levels [2].

4-2-3-Automatic exposure control (AEC):

Table 4-6 shows the automatic exposure control AEC measurement for three systems used in cardiology and fluoroscopic study. The result was within acceptable level of deviation in dose values at the image intensifier input surface. The variation in values was compared for three systems. The fluoroscopy unit in (AGH1) was better than (ANC) and (OHH) units.

4-2-4-Field limitation and source to skin distance:

The measurements were done for all systems. The results shown in Table 4-5, indicate that for all systems the field limitations were inside the image intensifier area and the shifts were similar for cardiology and IR systems.

Difference values of minimum source to skin distances were observed. All were well within the levels recommended [2].

4-2-5-Patient dose:

The results from Table 4-2 show that incident air kerma rate measured for standard phantom size of 20*20 cm^2 and for different sizes of PMMA and different image intensifier fields of view (7cm to 23 cm) for all fluoroscopy systems were within the international established guidance levels (50mGy/min - 100mGy/min) [20] for pulsed and continuous mode. This is with exception of (AGH2) where ESAK rates were larger. In the case of cine mode the doses were very high.

Consequently, the fluoroscopy units operators should avoid the cine and high pulsed and continuous modes of operation as much as possible to be within acceptable dose levels to patient with regard to image quality in the medical studies.

Comparison between doses obtained in this study with those reported in Ref [3], shows that the doses in this study are higher.

4-2-6-Limiting Resolution:

The results of image quality measurements in terms of limiting resolution shown in Table 4-4 indicate that for all systems the resolution was within recommended tolerance level [21].

The comparison between systems was done which showed that the resolution of cardiology systems is better than the fluoroscopy system; however this is all right, because in cardiology systems the resolution of system is more important than in fluoroscopy systems in the clinical applications.

4-2-7-Threshold contrast detail detectability:

The threshold contrast detail detectability TCDD was measured using TO10 contrast test tool to obtain the curves which were plotted as threshold detection index Vs square root area using fluoroscopy in some modes of operation. The Figures 4-1, 4-2, 4-3, 4-4, 4-5, and 4-6 show the contrast detail curves for fluoroscopy units in (ISH), (AGH1), (AGH2), (ANC), (OHH) and (ASH), respectively. These curves were in the logarithmic scale. The field of view for the TCDT was better for (ANC) unit. Tested fluoroscopy units have fields of view that vary from 19 to 23cm. Figure (4-7) indicated better contrast for (ANC) fluoroscopy unit followed by (AGH2), (ISH), (AGH1), (OHH) and (ASH), respectively.
The contrast curves were compared with the study reported in Ref [8]. However, the curves were of similar shapes and higher. The higher values of the curves indicate the contrast ability of the system.

4-2-8-Radiation protection:

Table 7 showed the numbers of the difference devices used in IR and fluoroscopic rooms the protect staff from scatter radiation in work. We noted that the staff used only aprons. However, gloves, screens, thyroid shield were not in use. Some of these centers protective aprons were very bad and corrupted but the numbers of it were good, more than 13 lead aprons in one room.
In the new systems and rooms the protection was well and the use of the devices were good.

Chapter five
Conclusion and recommendations

QC measurements were performed for six digital fluoroscopy systems. The results for incident air kerma rate measured for digital fluoroscopy are consistent with the recommended values when fluoroscopy is operated in pulsed mode. However, these values are often exceeded with continuous and cine modes. Therefore, operating fluoroscopy system at high doses modes should be avoided unless otherwise deemed necessary.

The kVp and HVL was well within the recommended values except in two systems that were affected in tube output and dose consistency.

Results from subjective image quality tests using standard Leeds test objects were compared between the systems (threshold contrast detail detectability and limiting spatial resolution). Spatial resolution was similar approximately between systems (between 1Lp/mm to 2Lp/mm) for fields of view between 19 to 23 cm.

The generation of TCDD curves from images of standard test objects is a simple procedure that allows analysis of image quality for a range of imaging modalities, including image intensifier systems. Threshold contrast data for a number of image intensifier systems have been presented for fluoroscopy images.

The measurement for image quality in terms of threshold contrast and limiting resolution were the first QC measurements of these systems. Because of this reason these TCDD curves can be used as the reference to evaluate the contrast in future QC measurements.

As the recommendation, fluoroscopy units operators should avoid the cine and high pulsed and continuous modes of operation as much as possible to be within acceptable dose levels to patient with regard to image quality in the medical studies.

References:

1. International Commission on Radiological Protection (2001) Avoidance of radiation injuries from medical interventional procedures. ICRP publication No.85.Pergamon Press, Oxford.

2. Suliman I I, van Soldt RTM and Zoetelief J. (2003). Protocol for quality control of equipment used in digital and interventional radiology. Delft University of Technology, Mekelweg 15, 2629 JB Delft, the Netherlands.

3. Suliman II, van Soldt RTM,Zoetelief J, Jansen J T M and Bosmans H (2005). Quality Control of equipment used in digital and interventional radiology. Rad. Prot. Dosim .117(1-3):277-282.

4. Suliman II, van Soldt, RTM, & Zoetelief J (2007). Digital fluoroscopy quality control measurements. In J Nagel & R Magjarevic (Eds.). IFMBE Proceedings, World Congress on Medical Physics and Biomedical Engineering. Seoul, South Korea 2006. Vol. 14: NUM 3, pp. 1470-1474. Springer, Berlin Heidelberg.

5. Connor U O, Dowling A, Gallagher A, Gorman D, Walsh C, Larkin A, Gray L, Devine M and Malone J(2008). Acceptance testing of fluoroscopy systems used for interventional purposes. St James's Hospital/the Haughton Institute, Dublin, Ireland. Published by Oxford University Press. All rights reserved.

6. Mary Beth Peter, Pavlicek W M S and Owen, J M(2000) Soft-Copy Quality Control of Digital Spot Images Obtained by Using X-ray Image Intensifiers. (Radiology, 216:810-819).

7. Padovani R, Trianni 0 A, Bokou C, Bosmans H, Jankowski J, Kottou S, Kepler K, Malone J, Tsapaki V, Salat D, Vano E and VassilevaJ(2008). Survey on performance assessment of cardiac angiography systems. Radiation Protection Dosimetry, Vol. 129, No. 1–3, pp (108–111).

8. EVAN DS , MACKENZIE A , LAWINSKI C P, MPHil and SMITH D, KCARE (2004).Threshold contrast detail detectability curve for fluoroscopy and digital acquisition using modern image intensifier system. The British Journal of Radiology, 77 (2004), 751–758 E. The British Institute of Radiology. DOI: 10.1259/bjr/16707499.

9. Walsh C, Dowling A, Meade A and Malone J (2005). Subjective and objective measurements of image quality in digital fluoroscopy. Radiation Protection Dosimetry, Vol. 117, No. 1–3, pp. 34–37.

10. Dimov A A, Vassileva J N (2008). Assessment of performance of new digital image intensifier fluoroscopy system. Radiation Protection Dosimetry 129(1-3):123-126.

11. Zoetelief J, Kottou S, Gray L, Salat D, Kepler K, Kaplanis P, Jankowski J, Schreiner A, and Vassileva J(2002-2006). Quality control measurements for fluoroscopy systems in eight countries participating in the sentinel EU coordinator action. Project co-funded by the European Commission under the Euratom Research and Training Programme on Nuclear Energy within the Sixth Framework Programme EUR 23105.

12. Camphausen K A, Lawrence R C (2008). Principles of Radiation Therapy, in Pazdur R, Wagman L D, Camphausen K A, Hoskins W J (Eds) Cancer Management: A Multidisciplinary Approach. 11 ed.

13. IAEA Tech.Rep.(2007), Dosimetry in diagnostic radiology: an interventional code of practice, Technical Report series No 457 (IAEA) pp: 20-25. IAEA, Vienna.

14. Finch, A. (2001) Assurance of quality in the diagnostic image department -2nd edition. Prepared by quality assurance working group of the radiation protection committee of the British Institute of Radiology, p.55.

15. Padovani R, Quai E, (2000). Comparison of Dosimetry Approaches in Interventional Radiology . FINAL REPORT, Ospedale S. Maria Della Misericordia, Udine, Italy. (www.dimond3.org).

16. Meade A D, Dowling A, Walsh C, Malone J F (2002). Draft proposal for three international standards for Dose Area Product (DAP) measurement, patient dose records and connectivity between equipment. (www.dimond3.org).

17. Final report of a coordinated research project (2006). Quantitative evaluation and promotion of patient dose limitation in fluoroscopically guided interventional procedures.

18. Tapiovaara M (2005). Image quality measurements in radiology. Radiation Protection Dosimetry, Vol. 117, No. 1–3, pp. 116–119.

19. International Electrotechnical Commission IEC (2000). International Standards 60601-2-43 Medical Electrical Equipment. Part 2-43: Particular Requirements for Safety of x-Ray Equipment for interventional Procedures. (Geneva: IEC).

20. Faulkner K (2001) Dose Display and Record Keeping. Radiat. Prot. Dosim. 94, 105-114.

21. Institute of Physics and Engineering in Medicine (2005). IPEM Report No. 77.

22. Recommended standard for the routine performance testing of diagnostic X-ray imaging systems (1997). IPEM Report 77.